2007 IEEE International Conference on
Robotics and Automation
Roma, Italy, 10-14 April 2007

Distance Estimation of Hidden Objects Based on Acoustical Holography by applying Acoustic Diffraction of Audible Sound

Haruhiko Niwa, Tetsuya Ogata, Kazunori Komatani, and Okuno G. Hiroshi

Abstract—**Occlusion is a problem for range finders; ranging systems using cameras or lasers cannot be used to estimate distance to an object (hidden object) that is occluded by another (obstacle). We developed a method to estimate the distance to the hidden object by applying acoustic diffraction of audible sound. Our method is based on time-of-flight (TOF), which has been used in ultrasound ranging systems. We determined the best frequency of audible sound and designed its optimal modulated signal for our system. We determined that the system estimates the distance to the hidden object as well as the obstacle. However, the measurement signal obtained from the hidden object was weak. Thus, interference from sound signals reflected from other objects or walls was not negligible. Therefore, we combined acoustical holography (AH) and TOF, which enabled a partial analysis of the reflection sound intensity field around the obstacle and hidden object. Our method was effective for ranging two objects of the same size within a 1.2 m depth range. The accuracy of our method was 3 cm for the obstacle, and 6 cm for the hidden object.**

I. Introduction

RANGE finder technology has become important, as automatic mobile robots are now common. Cameras and lasers are mainly used in this field. Camera range finder systems obtain details such as edge or color, however, they cannot be used under bad lighting conditions and require a high calculation cost [1, 2]. Laser range finder (LRF) systems can be used under various lighting conditions and require minimal calculation cost [3]. However, LRF systems are only used for high-accuracy range finders. Cameras and lasers are now often used together in range finder systems for different environments [4].

There systems have occlusion problems. When an object obscures others in the range of view, the distance to the hidden objects cannot be estimated using the systems previously described. This problem often exists in object tracking research. One current solution to this problem is, for example, to use multiple cameras. However, this is not practical if the measurement space is small.

We have tackled this problem by applying acoustic diffraction. Long-wavelength (low-frequency) waves diffract through wider angles than short-wavelength ones, so they will possibly reach the hidden object because they propagate around the obstacle. We used a low-frequency sound because of its operability or practicality. Our goal was to establish a basic method to estimate the distance to the hidden object using the audible sound.

Haruhiko Niwa, Tetsuya Ogata, Kazunori Komatani,, and Hiroshi G. Okuno are with Graduated School of Informatics, Kyoto University, Japan (niwa, ogata, komatani, okuno@lab5fs.kuis.kyoto-u.ac.jp).

Time-of-flight (TOF) is commonly used in sonar range finder systems [6]. High frequency sounds are transmitted as pulse-waveforms in TOF-based systems. An acoustic sensor receives the sound reflected from an object. The distance to the object is estimated from the time (named as "flight time") it takes the sound to reach the sensors. Our method is based on TOF. Usually ultrasound is used in TOF-based sonar range finders. We needed to test the ability of a range finder system using audible sound. Therefore, we determined the best frequency of the audible sound and designed its optimal modulated signal.

When we estimated the distance to the hidden object by this method, the signal-to-noise ratio (SNR) of the sound signal reflected from the hidden object was not intense enough in some cases. Thus interference from sound signals reflected from other objects or walls was not negligible. A sound directivity is low at long wavelengths, so this interference is unavoidable in our method. To improve the SNR, we must calculate the local reflection sound field around the obstacle and the hidden object. Acoustical Holography (AH) is a well-recognized technique used to do this. We combined AH and TOF to increase the SNR.

In section 2, we describe our measurement system and method. The configuration and parameters of our system are listed in section 3. The effectiveness of our method is verified by actual experiments described in section 4. Our method is discussed in section 5. The conclusion is in section 6.

II. Ranging System and Method

A. Measurement System

Our measurement system arrangement is illustrated in Figure (1). A burst wave defined by Equation (1) is transmitted from the sound source (speaker). The microphones receive sound reflected from the objects. The sound pressure measurement is described as *e*.

$$s(t) = \begin{cases} f(t) & (0 < t < T_b) \\ 0 & (t > T_b) \end{cases}, \tag{1}$$

where T_b is pulse duration. When one object is located in front of another directly in front of the microphones, the front one is called "obstacle" and back one "hidden object" in this paper.

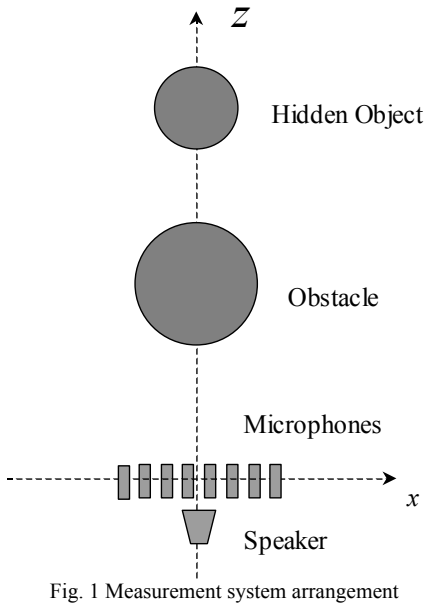

Fig. 1 Measurement system arrangement

B. Ranging method

(1) Cross-correlation function

Flight time T_0 of the reflected sound can be calculated with Equation (2) by applying a cross-correlation function to the measurement signal *e* and the transmission signal *s*.

$$r_{se}(\tau_m) = \sum_m e(t) \cdot s(t + \tau_m) , \quad (2)$$

where r_{se} is a correlation coefficient. If only one object is located in front of the microphones, T_0 can be calculated as follows,

$$T_0 = \arg\max_m \{r_{se}(\tau_m)\} . \quad (3)$$

Let τ_m be $md\tau$. The distance to the object is calculated as follows,

$$d_0 = cT_0 / 2 , \quad (4)$$

where *c* is sound velocity. If two objects are located as in Figure (1), the flight times T_0 and T_1 are obtained by finding two points that give local maximum values of r_{se}.

(2) Ranging method using AH

AH is an acoustical propagation equation based on the Helmholtz equation and a wave equation. It is used to calculate a complex sound pressure $P(u)$ at any position in front of the microphones and is obtained with Equation (5) using $P(u_p)$, which is measured .

$$P(u) = \int P(u_p) \exp[-\frac{jk_0}{z}(u_p - u)^2] du , \quad (5)$$

where *j* is an imaginary number, and k_0 is a wave number. Here, AH is used to calculate the reflected sound field within range S1, as shown in Figure (2). In this scenario, interference from other reflected sounds is reduced. $P(u_p)$ is defined with $e(u_p)$ as follows,

$$P(u, \tau_m) = \int_{\tau_m}^{\tau_m + T_{AH}} e(u_p) \exp(j2\pi f_0 t) dt . \quad (6)$$

The intensity of the reflected sound at time τ_m is defined as the maximum value of $P(u, \tau_m)$ in Equation (7).

$$P_{AH}(\tau_m) = \arg\max_{u \in S_1} \{P(u, \tau_m)\} . \quad (7)$$

Then Flight time T_0 is calculated as follows,

$$T_0 = \arg\max_m \{P_{AH}(\tau_m)\} . \quad (8)$$

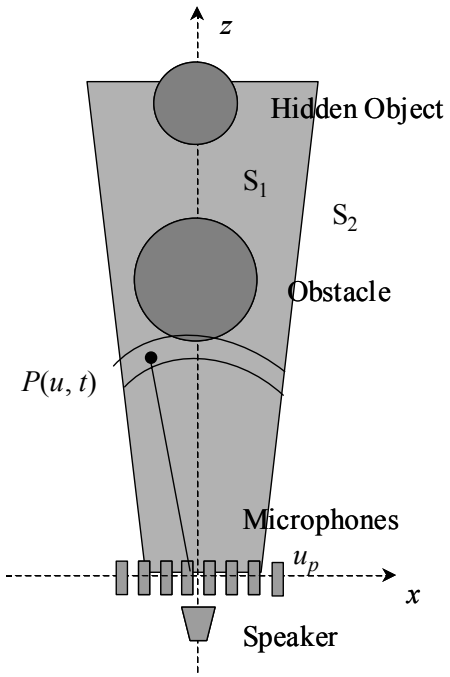

Fig. 2 Using AH

III. CONFIGURATION AND PARAMETER

Our ranging system was constructed with one speaker and eight microphones. Table (1) presents the configuration and parameters of our method and system. Note that our ranging resolution power was at most 1.42 cm, which was determined by the interval of TOF $d\tau$. The reconstructed space *S* set to be {-0.5 < *x*< 0.5} when the reflected sound field was visualized as an acoustic holography, and {-0.2 < *x*< 0.2} when the P_{AH} was calculated. Our computer model was a Pentium R4, 3-GHz PC/AT compatible.

Table 1 Configuration and Parameters

Specification of Sound Source or Data Acquisition	
Source Frequency	0.8 – 4.0 kHz
Sampling Frequency	48 kHz
Pulse Duration T_b	1.25 ms
Measurement Period T_c	14.5 ms
Interval of TOF $d\tau$	0.042 ms
Configuration of Measurement Plane	
Length of Measurement Plane	0.2 m
Number of Measurement Points	8
Parameter of AH Analysis	
Reconstructed Space S	$-0.5 < x < 0.5$ m $0.3 < z < 1.5$ m
Resolution of Reconstructed Space	x-axis: 200 z-axis: 30
Window Width T_{AH}	1.25 ms

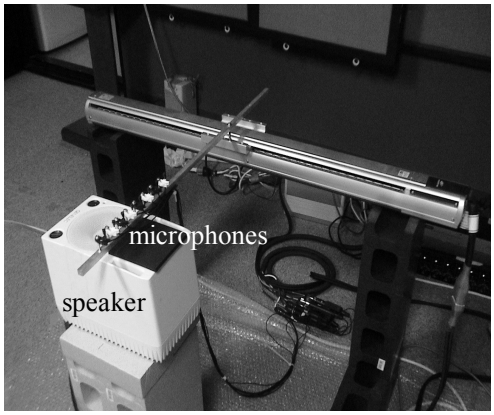

Fig. 3 Our ranging system

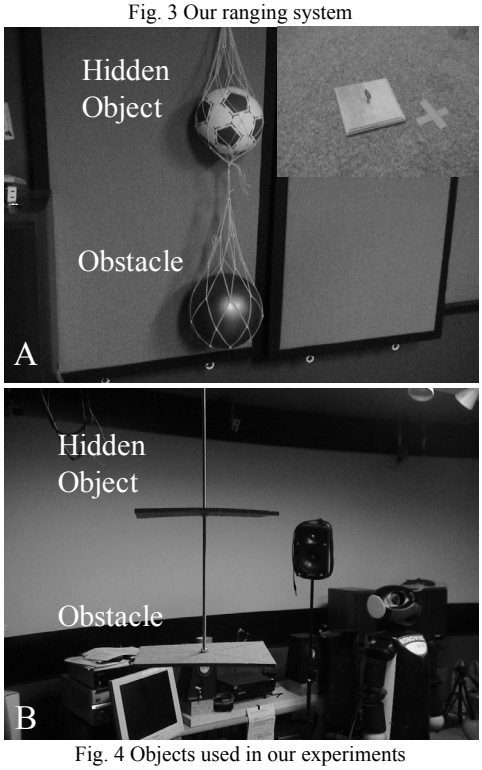

Fig. 4 Objects used in our experiments

The sound card was an M-audio Delta 1010, the speaker was a Generic 1029A and the microphone was a CONTRYMAN B3. The environment in which experiments were conducted is shown in Figure (3). The obstacles and hidden objects used in our experiments are shown in Figure (4).

IV. Experiment

We conducted two kinds of experiments as described in sections A and B. Note that limitations of our method in regard to obstacle shape and size were not investigated because an omni-directional sound source is more appropriate for investigating them. It is very difficult to manufacture such a source.

A. Performance of ranging system based on audible sound

Range finders based on low-frequency sound have poor distance resolution. However, the degree of acoustic diffraction will increase as sound frequency decrease. We determined a suitable frequency that enables ranging accurate to within 3 centimeters. We also designed an optimal modulated signal.

Experimental Conditions: A tabular object (plate) described in Figure (4-A) was located in front of the microphones as shown in Figure (4). The plate was 20 cm on each side. The distance from the plate to the microphone was changed between 0.5 and 1.2 m at 0.05-m intervals. We estimated distance d_0 using r_{se} or P_{AH}. r_{se} was calculated using the measurement signal obtained from Microphone 1, as shown in Figure 6. P_{AH} was calculated using measurement signals obtained from 8 microphones. When using r_{se}, we used 5 kinds of modulated signals defined as Equations (9-1) to (9-5).

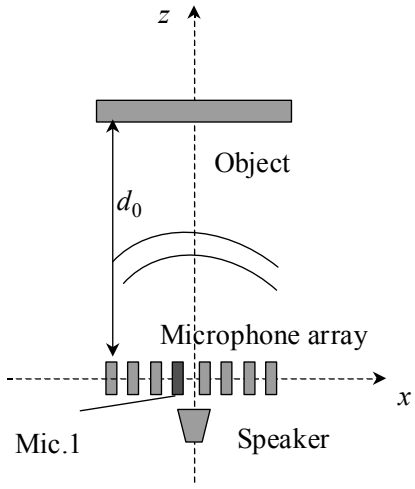

Fig. 5 Experiment 1

Pure tone: $f(t) = \sin(2\pi ft)$ (9-1)

AM: $f(t) = 0.5 \cdot (1 + \cos(2\pi f_a t)) \cdot \sin(2\pi ft)$ (9-2)

FM: $f(t) = \sin(2\pi ft + 8\sin(2\pi f_s t))$ (9-3)

Chirp: $f(t) = \sin(2\pi ft(1 + Bt))$ (9-4)

$$\text{BPSK: } f(t) = \begin{cases} \sin(2\pi ft) & 0 < t < 0.5T_b \\ \sin(2\pi ft + \pi) & 0.5T_b < t < T_b \end{cases}, \quad (9\text{-}5)$$

where f is basic frequency; it was alternated between 0.8, 1.6, 2.4, 3.2 and 4.0 kHz. We set f_a = 200, f_s = 200 and B = 500. When using P_{AH}, the source signal was pure tone because AH only works with stationary signals.

Results: Figure (6) presents the average and standard deviation values of errors for distances estimated from r_{se} using the pure tone signal. We determined that a 3.2-kHz sound is most suitable for this ranging method, whose resolution distance is smaller than 3 cm.

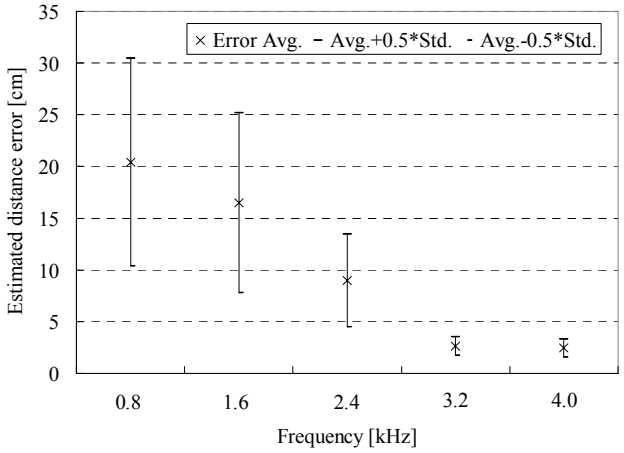

Fig. 6 Distance estimation using pure tone signal

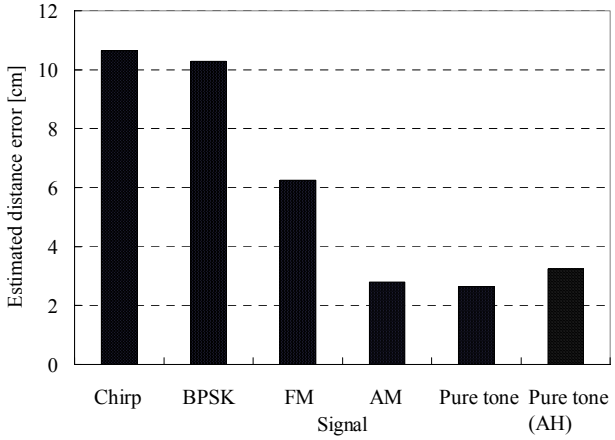

Fig. 7 Distance estimation using variant signals

Figure (7) presents average error values for distances estimated from r_{se} and P_{AH} by using the 5 modulated signals. Ranging accuracy worsened as the degrees of modulation of the source-signal frequency increased. If we had used ultrasound, this result should be opposite because linearity between the transmission and the measurement signals decreases due to sound reflecting from a 2-D surface when low-directivity sound is used. Range accuracy with P_{AH} was slightly worse than with r_{se}. We thought this was caused by sound constructive interference, which was not negligible when the target object surface was wide to some extent.

B. Range finder of the hidden object using r_{se} amd P_{AH}

We set two objects in front of the microphones with one hidden directly behind the other. First, we showed that SNR improved when we used P_{AH}. Next, the distance to the hidden object was estimated from P_{AH}. Then, we examined the accuracy of the estimated distance.

Experimental Conditions: A plate (described in Figure (4-B)) and a ball (described in Figure (4-A)) were located as shown in Figure (8). The plate was 20x20 cm, and the diameter of the ball is 20 cm. The objects were located as follows: d_1 was changed between 90 and 120 cm at 5 cm intervals by fixing d_0 at 50 cm, and d_0 was changed between 30 and 80 cm at 5 cm intervals by fixing d_1- d_0 at 40 cm. The number of measurement points was 11+7-1=17. The 3.2-kHz pure tone signal was used as the sound source. We estimated distance d'_1 to the hidden object with Equation (10), where we transformed r_{se} and P_{AH} into functions of d by using Equation (4). To compare r_{se} with P_{AH} appropriately, the microphone (1) described in Figure (8) was used for estimating d_1, because the microphone or microphone (8) could receive most sufficiently the sound reflected from the hidden object than other microphones.

$$d'_1 = \underset{d_0+0.3<d<1.4}{\arg\max} \{r_{se}(d) \; or \; P_{AH}(d)\} . \quad (10)$$

We determined ranging accuracy using d'_1.

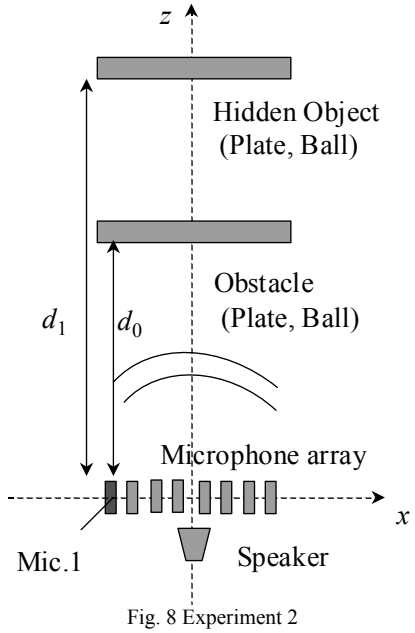

Fig. 8 Experiment 2

Results: Figure (9) shows r_{se} and P_{AH} when two balls were located at d_0 = 0.4 and d_1 = 0.8 m. The reflected sound signal from the hidden object was sufficiently obtained in r_{se} and P_{AH}. The SNR in P_{AH} was better than that in r_{se}. The intensity peak around at d = 1.6 m resulted from the wall of our experimental room.

Table (2) shows the accuracy results of d'_1. P_{AH} was used to

more high-accurate estimation of d_1 than r_{se}, especially when the ball was the obstacle. However, when the plate was the obstacle and the ball was the hidden object, d_1 could not be estimated by using P_{AH} or r_{se}. These results arise from degrees of acoustic diffraction, which depends on edge forms of target objects. Figure (10) presents P_{AH} when the two plate was located at (0.6, 1.0 m), (0.6, 1.1 m) and (0.6, 1.2 m). As shown in the figure, the peak of sound signal reflected from the hidden object was weak and gentle, although it indicates significantly the distance to the hidden objects.

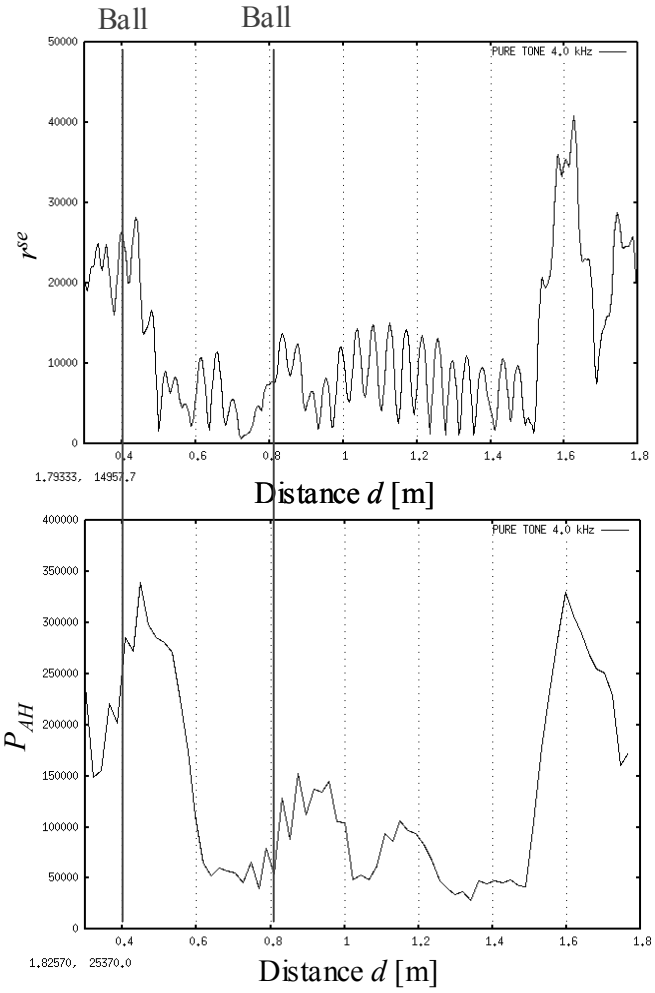

Fig. 9 r_{se} and P_{AH} for 2 balls located at 0.4 and 0.8 m

Table 2 Distance estimation using P_{AH}

Obstacle / Hidden Object	Plate / Plate	Plate / Ball	Ball / Plate	Ball / Ball
Avg. $\lvert d'_1 - d_1 \rvert$ (cm) P_{AH} /r_{se}	6.4/6.7	12.2/14.4	5.4/6.0	5.5/9.3

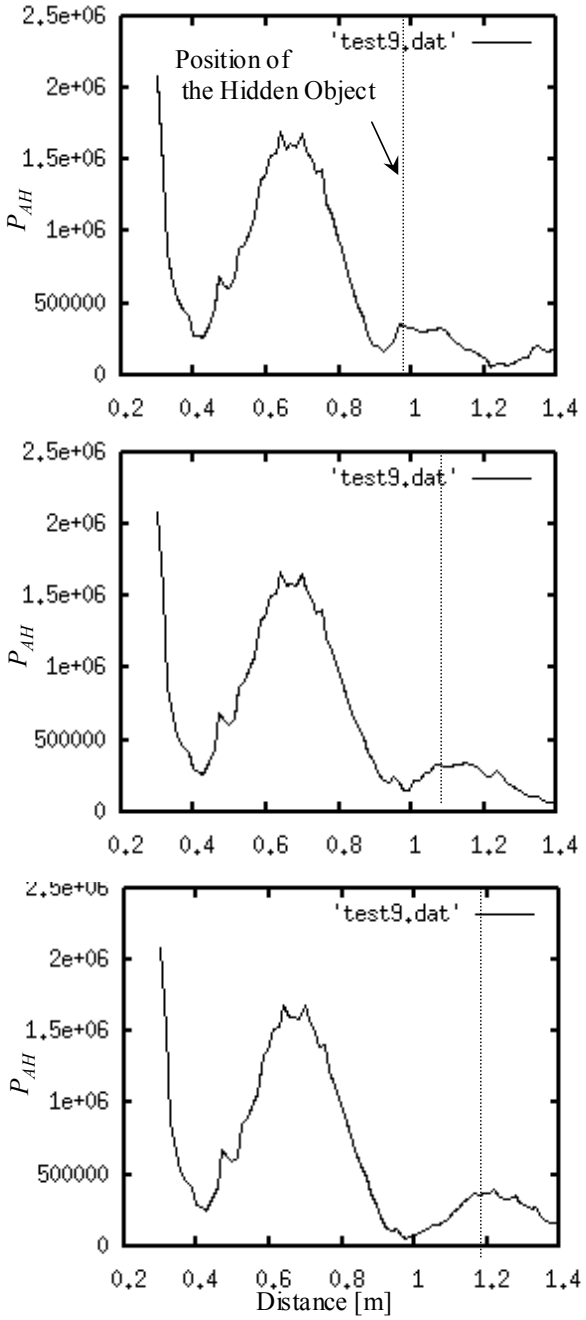

Fig. 10 r_{se} and P_{AH} for 2 balls located at 0.4 and 0.8 m

V. DISCUSSION

P_{AH} was a better ranging function than r_{se} for the SNR, it was not for ranging accuracy. The length of the measurement area has to be longer than the wavelength of the sound source when applying AH. From these perspectives, r_{se} might be a useful ranging function for small objects, and P_{AH} is suitable for estimating distances to objects hidden by a large obstacle, such as a wall. Furthermore, AH is generally used to analyze 3-D sound intensity fields. Holographs of reflected sound are shown in Figure (11).

From Figure (11), detection of the plate is better than that of the ball. This is due to the higher intensity of the reflected

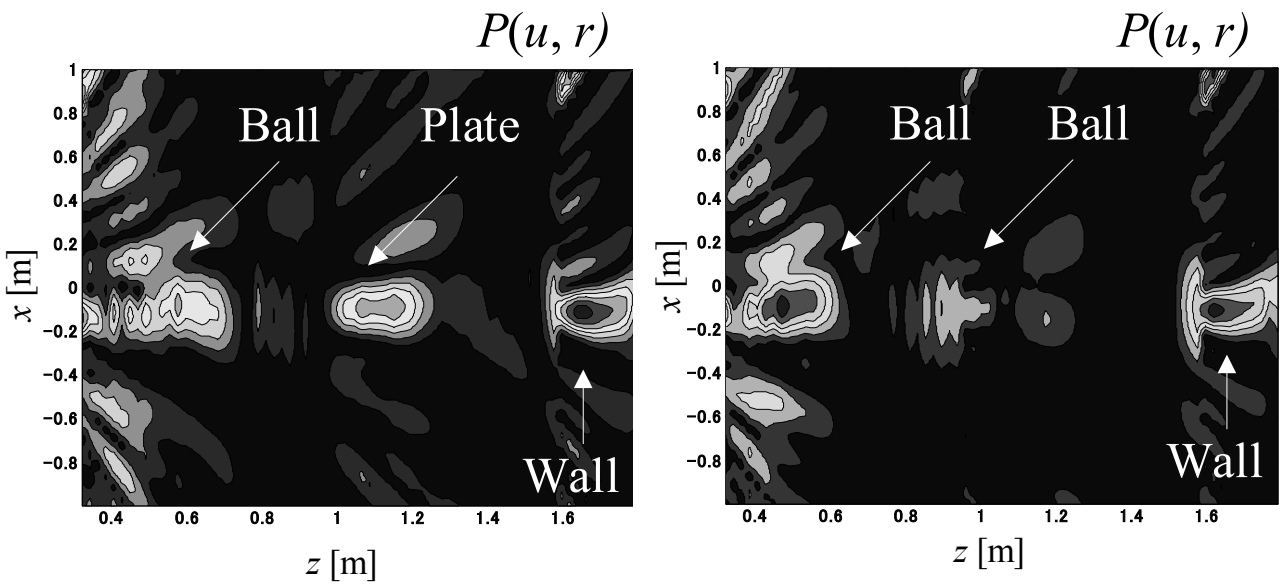

Fig. 11 Two-dimensional acoustical holographs of sound reflected from obstacle, object, and wall

sound arising from the planar surface of the plate, which bears high reflectance. Similarly, the wall is also visualized in the holography.

The holography contains noise in the vicinity (0.4m-0.6m of the z axis) of the obstacle. This results from the characteristic of the acoustical holography which is premised to apply for far-field sound intensity analysis. One means of resolving this issue is to integrate our method with NAH, which is used for near-field sound intensity analysis.

VI. Conclusion

We developed a method to estimate the distance to objects hidden by obstacles by using acoustic diffraction of audible sound. Time-of-flight with 3.2-kHz audible sound was used to estimate the distance to an object accurate to within 3 cm and the distance to an object hidden by an obstacle accurate to within 6 cm. Additionally the SNR of the measurement signal reflected from a hidden object was increased by combining AH and TOF. Our method was effective for estimating distances to two objects of the same size within a 1.2-m depth range.

We have been faced some issues; the distance to the hidden object cannot be estimated when assuming obstacles of variant shapes. We will investigate whether delayed sum is more practical for solving this problem than our current ranging method. Diffracted waves reach each microphone with some time delay. Delay time can be determined geometrically if the distance and size of an obstacle are obtained from a camera system. However, a high-frequency sampling (at least 192 kHz) sound card is needed to capture this time delay. Our current system does not have that capability. We will report about this approach in our next paper.

Reference

[1] Y. Zhang, Y. Sun, H. Sari-Sarraf, M. A. Abidi, "Impact of Intensity Edge Map on Segmentation of Noisy Range Images," Proc. of SPIE, 3958, 260-269 (2000)

[2] Y. Sun, C.Dumont, M. A. Abidi, "Mesh-based Integration of Range and Color Images," *Proc. Of SPIE AeroSense*, 4051, 110-117 (2000)

[3] H.Surmann, K.Lingemann, A.Nuchter and J.Hertzberg, "A 3D laser range finder for autonomous mobile robots," *Proc. the 32nd ISR*, 153-158 (2001)

[4] Yoshihiro, Negishi, Jun Miura, Yoshiaki Shirai, "Map Generation of a Mobile Robot by Integrating Omni directional Stereo and Laser Range Finder," *The Journal of Robotics Society of Japan*, 21–6, 690-696 (2003)

[5] A. Chaen, K. Yamazawa, N. Yokoya and H. Takemura, "Acquisition of Three-dimensional Information Using Omni Directional Stereo Vision," *Proc. Asian Conf. On Computer Vision*, 1, 288-295 (1998)

[6] C. Papageorgiou, C. Kosmatopoulos and T. Laopoulos, "Accurate Time-of-flight Measurement of Ultrasonic Signals for Displacement Monitoring Applications," *Proceeding of IEEE Instrument and Measurement Technology Conference*, 154-159 (1998)

[7] S. Ueha, "Acoustical Holography," *The Journal of the Acoustical Society of Japan*, 38-3, 166-169 (1982)

[8] M. Villot, G. Chaveriat and J. Roland, "An Acoustical Holography Technique for Plane Structures Radiating in Enclosed Spaces," *The Journal of Acoustical Society of America*, **91**, 187-195 (1992)

[9] J. D. Maynard, E. G. Williams and Y. Lee, "Near-field Acoustic Holography: I. Theory of Generalized Holography and the Development of NAH," *The Journal of Acoustical Society of America*, 78, 1395-1413 (1985)